LUND UNIVERSITY

Performance of a 28 GHz Two-Stage Rotman Lens Beamformer for Millimeter Wave Cellular Systems

Abbasi, Muhammad Ali Babar; Tataria, Harsh; Fusco, Vincent F ; Matthaiou, Michail

Link to publication

Performance of a 28 GHz Two–Stage Rotman Lens Beamformer for Millimeter Wave Cellular Systems

M. Ali Babar Abbasi, Harsh Tataria, Vincent F. Fusco and Michail Matthaiou

Institute of Electronics, Communications and Information Technology (ECIT), Queen's University Belfast, UK

e-mail: {m.abbasi, h.tataria, v.fusco, m.matthaiou}@qub.ac.uk

Abstract—**Phase shifter–based hybrid beamforming has received a lot of attention at millimeter–wave frequencies for cellular communications. Nevertheless, the implementation complexity of such beamformers is rather high due to the complexities involved in designing and fabricating the required radio–frequency (RF) circuits. In contrast, lens–based RF beamformers significantly reduce the implementation complexity, as all active circuits can be replaced by a passive device. In this paper, we present the sum spectral efficiency performance of an uplink multiuser multiple–input multiple–output (MU–MIMO) system with a 28 GHz Rotman lens. An asymmetric two–stage stacked design is fabricated with a 15 element (3×5) uniform rectangular array feeding 9 RF down–conversion chains towards baseband. Zero–forcing processing is employed at baseband for interference nulling and multistream recovery. Our results show that the MU–MIMO gains are substantially more pronounced for the two–stage architecture relative to a single–stage design due to the inclusion of the elevation multipath components. Moreover, we show that the asymmetric design can help to further reduce the implementation complexity, since the conventional beam selection network can be omitted from the RF front–end.**

I. INTRODUCTION

Beamforming is one of the most important concepts to efficiently mitigate the high propagation loss at millimeter–wave (mmWave) frequencies, and thus an integral part of future systems. The number of antenna elements in an array structure is proportional to the *directivity* of a beam created by the antenna array. The hardware development of mmWave beamformers and other radio–frequency (RF) front–end circuits include fundamental design challenges, and represent a bottleneck in meeting the theoretical potentials of multiuser multiple–input multiple–output (MU–MIMO) systems. Nevertheless, thanks to the small wavelengths at the mmWave frequencies, a large number of antenna elements can be packed within a relatively compact physical volume. Conventional MU-MIMO systems are built with a direct RF circuit between each antenna elements to the baseband processing, which requires *dedicated* up/down–conversion RF chains feeding each element. This is infeasible at mmWave frequencies due to the large number of antenna elements required in providing the necessary array gain. The number of *active* RF components can be lowered by transferring a *portion* of the processing towards the RF front–end leading to the popular *hybrid* beamforming approach [1–4]. A standard classical planar antenna array is capable only of forming a single beam, however to ensure uniform spatial *coverage* beam scanning capability is desired. To realize this, a pool of phase shifters is required

in the classical approach to implement hybrid beamformers which face two major design challenges. First, a phase shifter network pool is *lossy* at mmWave spectrum and requires a *separate* biasing network. Secondly, estimation of right angle-of-arrival (AOA), and projection of a beam towards the right angle-of-departure (AOD) needs high precision scanning. These two problems are complex and costly. Contemporaneous base–station (BS) arrays uses phase shifting networks [5, 6] thus are complex, especially in relation to re-producing for academic understandings.

Rotman lens–based beamformers pose a lucrative alternative. The primary reason for that is they use an analog beamforming network topology which combines the functionality of analog phase shifters, power dividers, and, in some cases, a combiners [7]. Lens–based beamformers also reduce the signal processing (SP) complexity of mmWave systems by associating fixed analog beams to a subset of the available RF chains, and consequently are particularly suitable for sparse mmWave channels to reduce the signal dimension in the RF domain. A standard Rotman lens provides a multibeam operation with a uniform linear array along the azimuth. The number of beams handled by a Rotman lens are equal to the number of beam–ports. The central region of the lens is where electromagnetic focusing takes place. Tapering lines and *phased-aligned* transmissions lines are used to connect the lens with the RF chains. Further details on the Rotman lens can be found in [8], while a theoretical model has been discussed in [9]. Unlike [9], in mmWave practical cellular scenario, scanning capability in both azimuth and elevation sector is required. In our work, we investigate and show the sum spectral efficiency of lens–based system by proposing two–stage stacked lens architecture (Fig. 1) for simultaneous azimuth and elevation sectoral coverage.

Contributions. We demonstrated a practical lens–based beamformer solution and prove two important capabilities of the proposed solution. Firstly, a system with required number of RF chains less than the number of antenna element is possible using lens–based analog phase shifting. This is possible because the number of beam–ports (N_{bp}) is allowed not to be equal to the number of array–ports (N_{ap}). Secondly, power combining from a two–dimensional (2–D) uniform rectangular array (URA) to a single RF input port is possible without the use of standard Wilkinson configuration. These two capabilities allow us to exclude the RF switching stage altogether, further reducing the hardware complexity. This is in
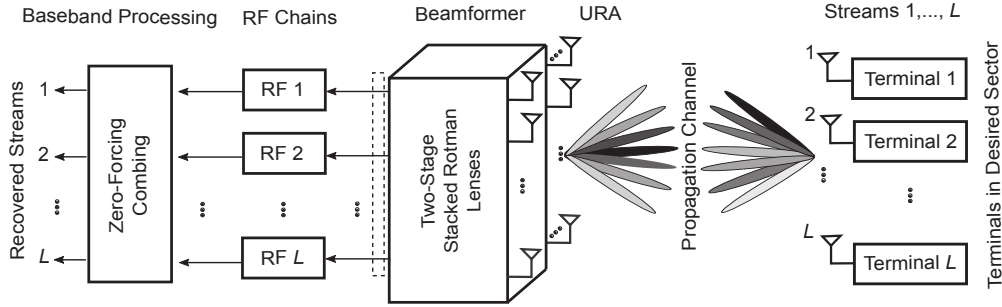
Fig. 1. Uplink MU-MIMO system model with a two–stage Rotman lens–based hybrid beamformer embedded receive URA.
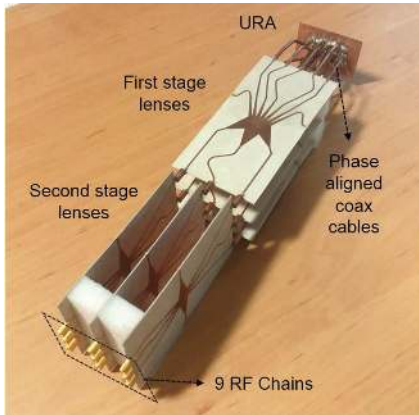

Fig. 2. Two–stage Rotman lens–based beamformer.

stark contrast to the existing lens state of the art where almost all works include the use of the practically challenging RF beam selection network. With ZF combining, we demonstrate the multi-stream separation of the system and estimated the spectral efficiency. Our results show that the fabricated Rotman lens structure achieves a significantly higher spectral efficiency than the simulated one–dimensional (1–D) Rotman lens. In addition to above, we propose an aggressive hardware reduction technique first by proposing an analog beamformer, reducing the cost and complexity of phase shifters, and secondly by proposing the beam port decimation that can further help in removing the requirement of switching matrix from the hybrid beamforming RF hardware.

II. SYSTEM MODEL

The hybrid architecture used in this study is presented in Fig. 1. We consider the uplink of a MU–MIMO system, where the BS array is equipped with two–stage Rotman lens–based beamformer. We used two stages of stacked printed circuit board (PCB) shown in Fig. 2 using the classical Rotman lens design principle. The first stage lens has $N_{ap} = 5$ and $N_{bp} = 3$, while the second stage lens has $N_{ap} = N_{bp} = 3$. All the lenses are fabricated on a 0.64 mm thick Taconic-RF 60 substrate ($\epsilon_r = 6.15$, $\tan(\delta) = 0.0038$) using *microstrip* technology. The first and second stage lenses are implemented the desired beamforming in the azimuth and elevation domains respectively. All lenses have two dummy–ports terminated to a 50 Ohm matched load [10]. The first stage lenses are connected to the 3×5 URA via *phase aligned* coax cables.

URA unit cells are operating at 28 GHz with a 10 dB bandwidth of 3650 MHz. The lens's parallel plate region is synthesized using tri-focal Rotman lens model [8, 11]. For the first stage lens, we have that the on-axis focal length $f_1 = 3\lambda$, on and off–axis focus length ratio $\beta = 0.9$, focal angle $\alpha = 30°$, sweep angle $\varphi_{max} = 40°$, and the array steering angle ϕ are set to $40°$. For the second stage lens, $f_1 = 2\lambda$, $\beta = 0.95$, $\alpha = 30°$, $\varphi_{max} = 30°$, to set a steering range θ of $15°$. The tapering lines for all the beam and array–ports are 3λ in length and are connected to 50 Ohm transmission lines. All the lines are phase aligned and are connecting the ports to the edge of the PCB. The expansion factor $\gamma = \sin(\varphi_{max}) / \sin(\alpha)$ and convex polygon [8] of both stage lens are chosen to ensure best operation at 28 GHz. Note that contrary to a classical hybrid architecture block, the RF switching network is missing from the uplink MU–MIMO system in Fig. 1. There is a specific reason for this. At the mmWave frequencies, RF switches are generally *lossy* and the insertion loss tends to increase as we move to higher frequencies. When multiple RF switches are cascaded to form a network, losses multiplies and degrades the overall system performance. Let alone the complexity, control biasing and cost, the scalability of the RF switching network at mmWaves is not as straightforward as that of the URA. This is primarily because of the availability of only discrete switching devices (like SP2T, SP4T etc.). Furthermore, in a mmWave MIMO cellular system, the switching matrix needs to be updated in every *coherence time* [12], increasing the implementation complexity further because of the transition time anomalies, switching speed, and thermal discharge. Due to these reasons, the proposed architecture (Fig. 1) eliminates completely the switching matrix by carefully handing over the beam selection capability directly to the two–stage stacked Rotman lens–based beamformer. With this, the beam–ports of the second stage lenses can directly be connected to the baseband SP unit via RF chains.

In our system model, the terminals are uniformly distributed within a $100°$ in azimuth and $30°$ in elevation sector, while the URA is situated at the origin of the sector area. Maximum coverage radius is assumed within this sector. URA with associated two–stage stack beam former is considered in receive mode covering both the azimuth and elevation zones. The URA receives uplink data streams from L user equipments (UEs). Each terminal transmits an independent data stream

to the URA with equal power in the same time–frequency resource. For simplicity, we assume a perfect knowledge of the propagation channel at both ends of the links. The uplink DOAs at the URA are assumed to be aligned with the intended beam directions by the two–stage beamformer. Due to the asymmetric design of the Rotman lens structure in both stages, the gain and phase on each URA element is down converted to L RF chains for baseband processing. The $L \times 1$ down–converted signal can be written as:

$$\mathbf{y} = \rho_\mathrm{t}^{\frac{1}{2}} \mathbf{F}_\mathrm{RF} \mathbf{H} \mathbf{x} + \mathbf{n} = \rho_\mathrm{t}^{\frac{1}{2}} \mathbf{G} \mathbf{x} + \mathbf{n}, \qquad (1)$$

where $\mathbf{G} = [\mathbf{g}_1 \ \mathbf{g}_2 \ \dots \mathbf{g}_L]$ is an $L \times L$ matrix such that the $L \times 1$ vector $\mathbf{g}_\ell = \mathbf{F}_\mathrm{RF} \mathbf{h}_\ell, \forall \ell = 1, 2, \dots, L$. The $M \times 1$ uplink channel vector for ℓ-th terminal is modeled as a *double–directional* finite multipath components (MPCs) response from [13], given by:

$$\mathbf{h}_\ell = \frac{1}{\sqrt{N_\mathrm{P}}} \sum_{p=1}^{N_\mathrm{P}} \alpha_{\ell,p} \, \Lambda\left(\phi_{\ell,p}, \theta_{\ell,p}\right) \mathbf{a}^H\left(\phi_{\ell,p}, \theta_{\ell,p}\right), \quad (2)$$

where N_P is the number of MPCs, while $\alpha_{\ell,p}$ models the gains of the p–th MPC, $\Lambda\left(\phi_{\ell,p}, \theta_{\ell,p}\right)$ denotes the per–antenna element gain, while $\mathbf{a}\left(\phi_{\ell,p}, \theta_{\ell,p}\right)$ is the far–field steering vector of the URA. *Instead of ideal DFT patterns, as routinely done in mmWave communication system literature, the measured patterns are then used for numerical evaluations.* Far-field patterns were measured in the Queen's University Belfast anechoic chamber facility (Fig. 3). It is noteworthy that the far–field patterns take into account the total focusing imperfections in the Rotman structure causing electromagnetic (EM) energy spill–over in the neighboring ports [14], and also capture the non–ideal power combining properties inside the lenses. The DOAs and the complex path attenuation models are assumed as uncorrelated with each other. Also, $\alpha_{\ell,p} \sim \mathcal{CN}\left(0, \beta_\ell\right)$ when $\beta_\ell = \zeta_\ell (r_\mathrm{ref}/r_\ell)^\chi$ captures large–scale fading impact within the channel, involving the shadow fading and geometric attenuations within the distance r_ℓ from the ℓ-th UE to the URA. In particular, $10 \log_{10}(\zeta_\ell) \sim \mathcal{CN}\left(0, \sigma_\mathrm{sf}^2\right)$, where σ_sf is the standard deviation of the shadow fading. Here r_ref is the reference distance from URA, while χ is the attenuation exponent. Moreover, the $\rho_\mathrm{t}^{1/2}\mathbf{x}$ is a $L \times 1$ vector of payload data in uplink when average transmit power of each terminal is given by ρ_t, with $\mathbb{E}[|x_\ell|^2] = 1, \forall \ell = 1, 2, \dots, L$. The net functionality lens–based beamformer when considering a perfect focusing capability is described by the $L \times M$ matrix:

$$\mathbf{F}_\mathrm{RF} = \left[\mathbf{a}^H(\phi_1, \theta_1) \ \mathbf{a}^H(\phi_2, \theta_2) \ \dots \ \mathbf{a}^H(\phi_M, \theta_M) \right]^T. \quad (3)$$

The $L \times 1$ vector of additive Gaussian noise is modeled as $\mathbf{n} \sim \mathcal{CN}(0, 1)$. We compare two cases. In the first case, we considered a 15 element uniform linear array (ULA) connected to a single–stage 1–D Rotman lens beamformer (see e.g. [14]) followed by 9 RF chains. In the second case, we replace this Rotman lens with the practical solution of URA connected to two–stage stacked Rotman lens–based beamformer directly connected to the 9 RF chains. Other than the beamformer, the remainder of the down conversion chains are considered perfect. This assumption is valid because of the fact that after

Fig. 3. Measurement setup in NSI anechoic chamber (photograph taken before covering the beamformer with absorbers).

the beamformer block, each L data streams have to have a dedicated RF chain (see Fig. 1). Any losses in these RF chains (LNA, mixer etc.) will remain the same for all UEs in uplink. At the baseband SP unit, the ZF processing nulls the multiuser interference, such that the SNR for a given ℓ-th user:

$$\mathrm{SNR}_\ell = \frac{\rho_\mathrm{t}}{\sigma^2 \left\{ \mathrm{Tr}\left[\left(\mathbf{G}^H \mathbf{G}\right)^{-1} \right]_{\ell,\ell} \right\}}, \qquad (4)$$

The ZF SNR for terminal ℓ can be projected to give an instantaneous spectral efficiency $\mathrm{R}_\ell = \log_2(1 + \mathrm{SNR}_\ell)$ in bit/sec/Hz. This has been used to compute the sum spectral efficiency of the system using:

$$\mathrm{R}_\mathrm{sum} = \sum_{\ell=1}^{L} \mathrm{R}_\ell. \qquad (5)$$

III. RESULTS AND DISCUSSION

The classical *double-directional description* [13] far-field propagation channel was simulated at 28 GHz. We consider 4 scattering clusters in the propagation channel when each cluster contributes a total number of 5 sub-paths. *Gaussian* distribution with zero-mean and unit variance is assumed for instantaneous path gains. Far-field array steering is in line with the $100°$ in azimuth and $30°$ in elevation coverage sector. Also, the elevation angular spread is Laplacian distributed while the azimuth angular spread is wrapped Gaussian, distributed from the central DOAs. Large-scale fading (geometric attenuation and shadow fading) is modeled using the classical power loss model described in [9]. Further information regarding the simulation setup, as well as the exact mathematical descriptions can be found in [9]. Final results are presented in Fig. 4. Note that in both cases of MIMO operation, each of the 9 RF chains need to be theoretically connected to all the antenna elements.

A two–stage Rotman lens–based beamformer considerably outperforms the 1–D counter part. This is mainly because of the addition of elevation component. The above trend is true at SNR = 5 dB as well as 15 dB, as can be observed from Fig. 4(a) and (b) respectively. Spectral efficiency calculations based on the measured results of two–stage Rotman lens–based
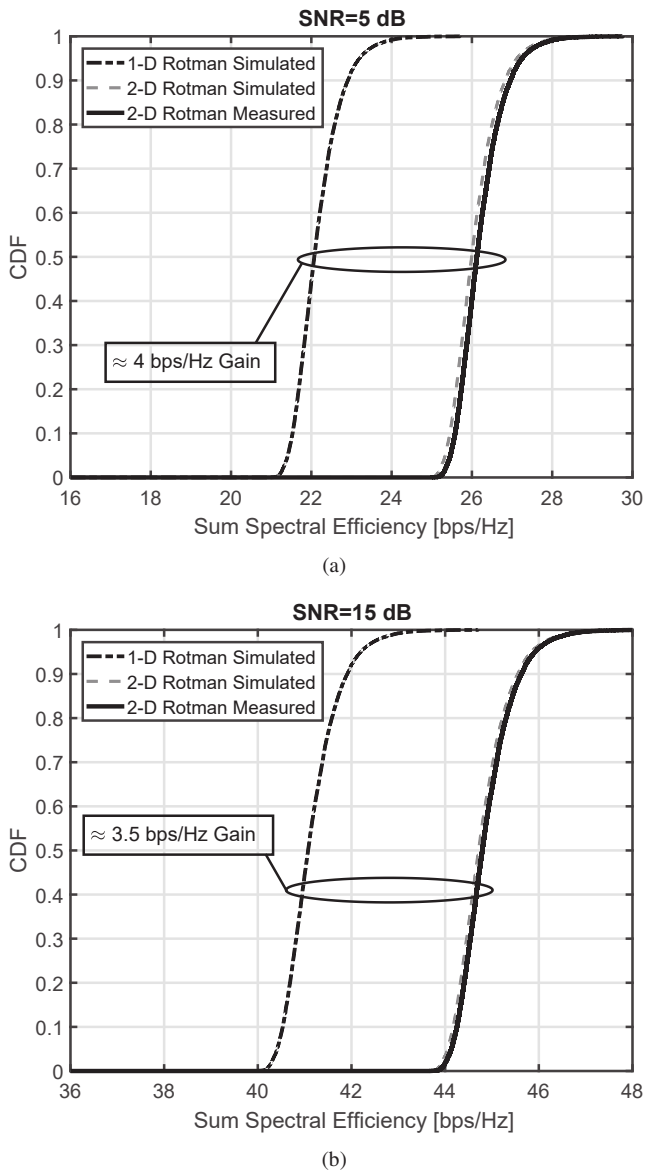
Fig. 4. Cumulative distribution function versus the SNR comparison when simulated single–stage (1–D), simulated and measured two–stage (2–D) Rotman lens–based beamformers were used at (a) SNR = 5 dB and (b) SNR = 15 dB.

beamformer matches very well with the simulated predictions based on a full–wave EM and circuit solver, ensuring the practicality of the approach. The proposed hybrid architecture is scalable. For instance, to support a 64 antenna element URA in 8×8 formation connected to 16 RF chains, a total number of 12 1–D Rotman lenses is required. Assembled in the same fashion as shown in Fig. 2, we need 8 horizontally stacked lenses to form the first stage and 4 vertically stacked for the second stage. Both stage lenses need to have $N_{ap} = 8$ and $N_{bp} = 4$. Similar formation can be synthesized for a URA with un–equal rows versus column antenna elements. Also, any number of N_{ap} to N_{bp} combination tailored to specific requirements is possible as long as N_{ap} and $N_{bp} > 3$, ensuring the design simplicity with an added benefit of aggressive hardware reduction.

IV. Conclusion and Future Prospects

A two–stage Rotman lens–based beamformer is proposed and evaluated in an attempt to propose a significant reduction in the implementation complexity and cost of a mmWave MIMO hybrid architecture radio front–end. The sum spectral efficiency performance of uplink MU–MIMO system is evaluated with a 28 GHz asymmetric beamformer hardware based on Rotman lenses. A total number of 6 Rotman lens are fabricated, strategically stacked and connected to URA capable of covering $\phi = -40°$ to $+40°$ and $\theta = -15°$ to $+15°$ BS sector. Practically, MU–MIMO +gain of ∼4 dB at SNR = 5dB and ∼3.6 dB at SNR = 5dB is anticipated when comparing the devised two–stage to a simulated single–stage lens–based beamformer architecture. Approximately similar trend is expected if the same design topology is re–scaled. The evaluated proof–of–concept hardware can be treated as a *brick* of a scaled system. A fully connected BS demonstrator realizing massive–MIMO to support a larger number of antenna array is one of our future directions.

References

[1] V. Raghavan, *et al.*, "Beamforming tradeoffs for initial UE discovery in millimeter-wave MIMO systems," *IEEE J. Sel. Topics Signal Process.*, vol. 10, no. 3, pp. 543-559, Apr. 2016.

[2] A. M. Sayeed and J. Brady, "Beamspace MIMO channel modeling and measurement: Methodology and results at 28 GHz," in *Proc. IEEE GLOBECOM (Workshops)*, Dec. 2016.

[3] Y. Zeng, L. Yang, and R. Zhang, "Multi-user millimeter-wave MIMO with full-dimensional lens antenna arrays," *IEEE Trans. Wireless Commun.*, vol. 17, no. 4, pp. 2800-2814, Apr. 2018.

[4] T. Kwon, *et al.*, "RF lens-embedded massive MIMO systems: Fabrication issues and codebook design," *IEEE Trans. Microwave Theoy Techn.*, vol. 64, no. 7, pp. 2256-2271, Jul. 2016.

[5] W. Hong, *et al.*, "Multibeam antenna technologies for 5G wireless communications," *IEEE Trans. Antennas Propag.*, vol. 65, no. 12, pp. 6231-6249, Dec. 2017.

[6] A. F. Molisch, *et al.*, "Hybrid beamforming for massive MIMO: A survey," *IEEE Commun. Mag.*, vol. 55, no. 9, pp. 134-141, Sep. 2017.

[7] B. Yang, *et al.*, "Digital beamforming-based massive MIMO transceiver for 5G millimeter-wave communications," *IEEE Trans. Microwave Theory Techn.*, vol. 66, no. 7, pp. 3403-3418, Jul. 2018.

[8] R. C. Hansen, "Design trades for Rotman lenses," *IEEE Trans. Antennas Propag.*, vol. 39, no. 4, pp. 464-472, 1991.

[9] H. Tataria, *et al.*, "Uplink interference analysis with RF switching for lens–based millimeter–wave systems", in *Proc. IEEE ICC*, Kansas City, MO, May 2018, pp. 1-7.

[10] Vihay Dale RF/High Frequency Products, "High Frequency 50 GHz Thin Film Chip Resistor, " CH0402 datasheet, [Revised Feb. 2018].

[11] Y. Gao, *et al.*, "Rotman lens based hybrid analog-digital beamforming in massive MIMO systems: Array architectures, beam selection algorithms and experiments," *IEEE Trans. Veh. Technol.*, vol. 66, no. 10, pp. 9134-9148, Oct. 2017.

[12] E. G. Larsson, *et al.*, "Antenna count for massive MIMO: 1.9 GHz versus 60 GHz," *IEEE Commun. Mag.*, vol. 56, no. 9, pp. 132-137, Sep. 2018.

[13] M. Steinbauer, *et al.*, "The double-directional radio channel," in *IEEE Antennas Propag. Mag.*, vol. 43, no. 4, pp. 51-63, Aug 2001.

[14] M. A. Babar Abbasi, *et al.*, "On the impact of spillover losses in 28 GHz Rotman lens arrays for 5G applications," in *Proc. 2018 IEEE MTT-S IMWS-5G*, Oct. 2018.